Projections of Annual Mean Air Temperature and Precipitation over the Globe and in China During the 21st Century by the BCC Climate System Model BCC_CSM1.0

ZHANG Li* (张 莉), WU Tongwen (吴统文), XIN Xiaoge (辛晓歌), DONG Min (董 敏), and WANG Zaizhi (王在志)

Division of Climate System Modeling & Laboratory for Climate Studies, National Climate Center, China Meteorological Administration, Beijing 100081

(Received March 30, 2011; in final form January 4, 2012)

ABSTRACT

Evaluating the projection capability of climate models is an important task in climate model development and climate change studies. The projection capability of the Beijing Climate Center (BCC) Climate System Model BCC_CSM1.0 is analyzed in this study. We focus on evaluating the projected annual mean air temperature and precipitation during the 21st century under three emission scenarios (Special Report on Emission Scenarios (SRES) B1, A1B, and A2) of the BCC_CSM1.0 model, along with comparisons with 22 CMIP3 (Coupled Model Intercomparison Project Phase 3) climate models. Air temperature averaged both globally and within China is projected to increase continuously throughout the 21st century, while precipitation increases intermittently under each of the three emission scenarios, with some specific temporal and spatial characteristics. The changes in globally-averaged and China-averaged air temperature and precipitation simulated by the BCC_CSM1.0 model are within the range of CMIP3 model results. On average, the changes of precipitation and temperature are more pronounced over China than over the globe, which is also in agreement with the CMIP3 models. The projection capability of the BCC_CSM1.0 model is comparable to that of other climate system models. Furthermore, the results reveal that the climate change response to greenhouse gas emissions is stronger over China than in the global mean, which implies that China may be particularly sensitive to climate change in the 21st century.

Key words: BCC_CSM1.0, air temperature, precipitation, projection

Citation: Zhang Li, Wu Tongwen, Xin Xiaoge, et al., 2012: Projections of annual mean air temperature and precipitation over the globe and in China during the 21st century by the BCC Climate System Model BCC_CSM1.0. *Acta Meteor. Sinica*, **26**(3), 362–375, doi: 10.1007/s13351-012-0308-8.

1. Introduction

Global climate change characterized by global warming has been occurring over the past 100 years and is still evolving. The non-negligible impacts of this change have deeply affected the global natural ecosystem and economy. Dealing with the issues associated with climate change has become a considerable focus of governments. The Chinese government has instituted multiple programs centered on the scientific projection of future climate change, including the National Climate Change Program and the Scientific and Technological Actions on Climate Change.

Scientific projections of future climate change are essential for developing strategies to adapting to or coping with climate change. As part of the Intergovernmental Panel on Climate Change (IPCC) Fourth Assessment Report (AR4) (IPCC, 2007), scientists were organized to evaluate the ability of climate models in simulating climate and climate change. Future climate change can be projected on both global and regional scales using the multi-model ensemble. Numerical experiments are performed under a series of possible future scenarios according to idealized emis-

Supported by the National Science and Technology Support Program of China (2007BAC03A01 and 2007BAC29B03), National Basic Research and Development (973) Program of China (2010CB951902), and China Meteorological Administration Special Public Welfare Research Fund (GYHY200806006).

*Corresponding author: zhangli@cma.gov.cn.

sions or assumed concentration levels, based mainly on the Special Report on Emission Scenarios (SRES) (Nakicenovic et al., 2000).

The multi-model projection of air temperature and precipitation over China from the IPCC AR4 (IPCC, 2007) has been analyzed by a number of Chinese scholars (Li and Zhou, 2010; Li et al., 2011; Feng et al., 2010; Jiang et al., 2008; Zhang, 2008; Xu et al., 2005). The results of these and other studies using the AR4 multi-model ensemble show that global surface and tropospheric air temperatures will continue to increase under three emission scenarios (SRES A2, A1B, and B1) throughout the 21st century (IPCC, 2007), while stratospheric air temperatures may decrease. Globally-averaged precipitation is generally projected to increase, with changes at high latitudes more coherent among the individual models. China is likely to become significantly warmer, with a projected temperature increase of approximately 3.5℃ by the end of the 21st century. This warming is projected to be greater in the north of China and less in the south. Precipitation is projected to increase by about 7.5% by the end of the 21st century (Jiang et al., 2008; Xu et al., 2005). However, the projections of both air temperature and precipitation have large uncertainties on the regional scale (Li and Zhou, 2010; Li et al., 2011; Feng et al., 2010).

The development of climate system models has progressed significantly, especially since the publication of the IPCC Third Assessment Report (IPCC, 2001) (Wang et al., 2009). Both the climate model BCC_CM1 developed by the Beijing Climate Center (BCC) of the China Meteorological Administration (CMA) and the climate system model FGOALS-g1.0 developed by the Institute of Atmospheric Physics (IAP) of the Chinese Academy of Sciences participated in the IPCC AR4. The IAP has developed coupled climate system models FGOALS_s and FGOALS_g, which use the Spectral Atmospheric General Circulation Model (AGCM) of IAP/LASG (SAMIL) and the Grid-point Atmospheric Model of IAP/LASG (GAMIL), respectively (Zhou et al., 2005a, b, 2007, 2008; Yu et al., 2008). These models are able to reproduce historical climate over the globe and in China to some extent. The National Climate Center/BCC of China began to develop a climate system model BCC_CSM in 2004 (Wu et al., 2010a, b), which is independent of BCC_CM1. The evaluation of BCC_CSM1.0 shows that the model is able to capture many of the main characteristics of historical climate (Xin et al., 2009; Dong et al., 2009). At present, NCC and IAP are using their respective new versions of climate system models to participate in the IPCC 5th Assessment Report (AR5) and Coupled Model Intercomparison Project Phase 5 (CMIP5).

The capabilities of coupled models were evaluated in IPCC AR4 using simulations of historical climate in the 20th century and projections of future climate change. Zhou and Yu (2006) comprehensively analyzed the abilities of 19 coupled models in simulating global and Chinese surface air temperature. Zhang (2008) analyzed the abilities of these same models in simulating precipitation over East Asia. The results show that, although the majority of the coupled models are able to capture the basic characteristics of regional climate in the 20th century, there are still large uncertainties in the simulation results.

In this paper, we focus on the evaluation of projected changes in air temperature and precipitation during the 21st century under SRES B1, A1B, and A2 by the BCC_CSM1.0 and 22 other coupled models that participated in CMIP3. This study intends to evaluate the projection capability of BCC_CSM1.0 and improve understanding of future climate scenarios and the uncertainties in the projections. The data and models are introduced in detail in Section 2. The main results of projected temperature and precipitation over China are presented in Section 3. The conclusions and discussion are given in Section 4.

2. Model and data

2.1 Model introduction

The BCC of the CMA began to develop the new generation multi-sphere climate system model BCC_CSM in 2004, and has since built a number of different versions. The climate system model version 1 (BCC_CSM1.0) is based on the CCSM2.0 (Kiehl

and Gent, 2004) developed by the National Center for Atmospheric Research (NCAR) of the United States. The differences between BCC_CSM1.0 and CCSM2.0 are mainly in the atmosphere and land components of the model. BCC_CSM1.0 comprises the BCC_AGCM2.0.1 atmospheric model (Wu et al., 2010a, b), the Community Land Surface Model version 3 (CLM3) (Dickinson et al., 2006), the Parallel Ocean Program (POP), and the Community Sea Ice Model version 4 (CSIM4) (Briegleb et al., 2004). These individual components are coupled using the CPL5 (Coupler version 5) coupling system (Kauffman, 2002). Zhou et al. (2004) described the characteristics and development of CPL5 in detail.

BCC_AGCM2.0.1 is a spectral model with T42 truncation (a horizontal resolution of about 2.8125°) and 26 vertical layers. It performs well in simulating the basic climate of precipitation, temperature, thermal structure, atmospheric circulation (Wu et al., 2010a, b), intraseasonal oscillations of zonal wind and precipitation (Dong et al., 2009), and the Asian-Australian monsoon (Wang et al., 2009). The ocean model POP has 40 vertical levels and tripolar grids in the horizontal. The longitudinal resolution is approximately 1° and the latitudinal resolution is variable with finer resolution (∼0.3°) near the equator.

In general, BCC_CSM1.0 is able to reflect the characteristics of historical climate to some extent (e.g., DCSM, 2008; Zhang et al., 2011). The model can capture the spatial distribution of climatic mean precipitation and partly reproduce some of the centers of heavy rain, such as those in the tropical western Pacific, the Bay of Bengal, and the western Indian Peninsula. There are also some biases in the model, such as excess precipitation over the subtropical Pacific, the Qinghai-Tibetan Plateau, and the Arabian Sea, and insufficient precipitation over the Bay of Bengal, Indonesia, and the tropical Atlantic. BCC_CSM1.0 is able to capture the basic characteristics of the temperature distribution, with the following biases relative to the NCEP/NCAR reanalysis data: higher air temperature over land and lower air temperature over the Pacific and Atlantic oceans in the Northern Hemisphere. In general, BCC_CSM1.0 captures many of the characteristics of historical climate.

In this study, we focus on the following key questions. How good is the projection capability of BCC_CSM1.0? What are the projected changes in temperature and precipitation over the globe and in China? What are the similarities and differences in the projections between BCC_CSM1.0 and other models? The outputs of 22 other climate system models that contributed to CMIP3 are used for comparison. The details of these models are listed in Table 1, with additional information available at http://www-pcmdi.llnl.gov/ipcc/model documentation/ipcc_model_documentation.php.

In order to evaluate the capability of BCC_CSM1.0 in projecting future climate, numerical experiments forced by three emission scenarios (i.e., SRES B1, A1B, and A2) as used in the experiments of IPCC AR4 were carried out.

2.2 Data

This paper analyzes projections of monthly air temperature and precipitation in the 21st century under SRES B1, A1B, and A2 by BCC_CSM1.0 and 22 other climate system models that have participated in CMIP3. The details of the data are listed in Table 2.

The ensemble mean is calculated by interpolating the results from all of the models onto a uniform horizontal resolution (1° latitude ×1° longitude). Anomalies are calculated relative to the 30-yr mean from 1961 to 1990.

3. Results

3.1 Annual mean surface air temperature change in the 21st century

3.1.1 Globally-averaged annual mean surface air temperature

Figure 1a shows the temporal variations of globally-averaged annual mean surface air temperature in the 21st century projected by BCC_CSM1.0 under SRES B1, A1B, and A2. Warming of surface air temperature during the 21st century is continuous

Table 1. General information on the climate models

IPCC model I.D.	Institution	Atmospheric model resolution	Ocean model resolution
BCC_CSM1.0	BCC	T42(∼2.8°×2.8°) L26	0.3°–1°×1° L40
BCCR-BCM2.0	BCCR	T63 (1.9°×1.9°)	0.5°–1.5°×1.5° L35
CCSM3	NCAR	T85 (1.4°×1.4°) L26	0.3°–1°×1° L40
CGCM3.1(T47)	CCCma	T47 (∼2.8°×2.8°) L31	1.9°×1.9° L29
CGCM3.1(T63)	CCCma	T63 (∼1.9°×1.9°) L31	0.9°×1.4° L29
CNRM-CM3	CNRM	T63 (∼1.9°×1.9°) L45	0.5°–2°×2° L31
CSIRO-Mk3.0	CSIRO	T63 (∼1.9°×1.9°) L18	0.8°×1.9° L31
ECHAM5/MPI-OM	MPI	T63 (∼1.9°×1.9°) L31	1.5°×1.5° L40
ECHO-G	MIUB/MRI	T30 (∼3.9°×3.9°) L19	0.5°–2.8°×2.8° L20
FGOALS-g1.0	IAP	T42 (∼2.8°×2.8°) L26	1.0°×1.0° L16
GFDL-CM2.0	GFDL	2.0°×2.5° L24	0.3°–1.0°×1.0°
GFDL-CM2.1	GFDL	2.0°×2.5° L24	0.3°–1.0°×1.0°
GISS-AOM	GISS	3°×4° L12	3°×4° L16
GISS-EH	GISS	4°×5° L20	2°×2° L16
GISS-ER	GISS	4°×5° L20	4°×5° L13
INM-CM3.0	INM	4°×5° L21	2°×2.5° L33
IPSL-CM4	IPSL	2.5°×3.75° L19	2°×2° L31
MIROC3.2(hires)	UT,JAMSTEC	T106 (∼1.1°×1.1°) L56	0.2°×0.3° L47
MIROC3.2(medres)	UT,JAMSTEC	T42 (∼2.8°×2.8°) L20	0.5°–1.4°×1.4° L43
MRI-CGCM2.3.2	MRI	T42 (∼2.8°×2.8°) L30	0.5°–2.0°×2.5° L23
PCM	NCAR	T42 (∼2.8°×2.8°) L26	0.5°–0.7°×1.1° L40
UKMO-HadCM3	UKMO	2.5°×3.75° L19	1.25°×1.25° L20
UKMO-HadGEM1	UKMO	∼1.3°×1.9° L38	0.3°–1.0°×1.0° L40

Table 2. Data availability under different simulation scenarios

NO.	IPCC model I.D.	SRES B1			SRES A1B			SRES A2		
		SAT	AT	Pr	SAT	AT	Pr	SAT	AT	Pr
1	BCC_CSM1.0	Y	Y	Y	Y	Y	Y	Y	Y	Y
2	BCCR-BCM2.0	Y	Y	Y	Y	Y	Y	Y	Y	Y
3	CCSM3	Y	Y	Y	Y	Y	Y	Y	Y	Y
4	CGCM3.1(T47)	Y	Y	Y	Y	Y	Y	Y	Y	Y
5	CGCM3.1(T63)	Y	Y	Y	Y	Y	Y	N	N	N
6	CNRM-CM3	Y	Y	Y	Y	Y	Y	Y	Y	Y
7	CSIRO-Mk3.0	Y	Y	Y	Y	Y	Y	Y	Y	Y
8	ECHAM5/MPI-OM	Y	Y	N	Y	Y	N	Y	Y	N
9	ECHO-G	Y	N	Y	Y	N	Y	Y	N	Y
10	FGOALS-g1.0	Y	Y	Y	Y	Y	Y	N	N	N
11	GFDL-CM2.0	Y	Y	Y	Y	Y	Y	Y	Y	Y
12	GFDL-CM2.1	Y	Y	Y	Y	Y	Y	Y	Y	Y
13	GISS-AOM	Y	Y	Y	Y	Y	Y	N	N	N
14	GISS-EH	N	N	N	Y	Y	Y	N	N	N
15	GISS-ER	Y	N	Y	Y	Y	Y	Y	N	Y
16	INM-CM3.0	Y	Y	Y	Y	Y	Y	Y	Y	Y
17	IPSL-CM4	Y	Y	Y	Y	Y	Y	Y	Y	Y
18	MIROC3.2(hires)	Y	Y	Y	Y	Y	Y	N	N	N
19	MIROC3.2(medres)	Y	Y	Y	Y	Y	Y	Y	Y	Y
20	MRI-CGCM2.3.2	Y	Y	Y	Y	Y	Y	Y	Y	Y
21	PCM	Y	Y	Y	Y	Y	Y	Y	Y	Y
22	UKMO-HadCM3	Y	Y	Y	Y	Y	Y	Y	Y	Y
23	UKMO-HadGEM1	N	N	N	Y	Y	Y	N	N	N

Notes: Y: data are available; N: no data. SAT: surface air temperature; AT: air temperature; Pr: precipitation.

under each of the three emission scenarios. The warming rate under SRES A2 is 0.31℃ (10 yr)$^{-1}$, larger than the other two scenarios; the rate under B1 is 0.17℃ (10 yr)$^{-1}$, smaller than the other two scenarios. The rate under SRES A1B is 0.23℃ (10 yr)$^{-1}$. By the late 21st century (2080–2099), the amplitude of the warming is the highest under SRES A2 (about 3.24℃). The warming is least pronounced under SRES B1 (about 1.99℃), and moderate under SRES A1B (about 2.63℃).

Table 3 lists the rates of 21st century warming and the amounts of warming by the late 21st century for annual mean surface air temperature averaged globally and over China under the different emission scenarios. Comparison of these results shows that the BCC_CSM1.0 projection is within the range of the CMIP3 model results. The multi-model ensemble mean gives a projected 21st century warming rate and amplitude of 0.33℃ (10 yr)$^{-1}$ and 3.27℃, respectively, under the A2 scenario, largest among the three emission scenarios. The rate and amplitude under the B1 case are 0.17℃ (10 yr)$^{-1}$ and 1.96℃, respectively, smallest among the three scenarios. For the A1B case, the projected warming rate is 0.28℃ (10 yr)$^{-1}$, and the amplitude is 2.82℃. The BCC_CSM1.0 results are quite consistent with the multi-model ensemble means.

3.1.2 Annual mean surface air temperature averaged over China

Figure 1b shows the time series of regionally-averaged annual mean surface air temperature over China under SRES B1, A1B, and A2 as simulated by BCC_CSM1.0. The projected warming of surface air temperature under each emission scenario is continuous throughout the 21st century. The warming rate and amplitude under SRES A2 are 0.42℃ (10 yr)$^{-1}$ and 4.36℃, respectively, larger than those under the other two scenarios. The values under SRES B1 are 0.20℃ (10 yr)$^{-1}$ and 2.52℃, respectively, smallest of the three scenarios, and those under SRES A1B are 0.30℃ (10 yr)$^{-1}$ and 3.33℃, respectively. The warming averaged over China is greater than the corresponding global mean.

A comparison of the BCC_CSM1.0 results (Table 3) with the results from other models shows that the BCC_CSM1.0 projection is within the range of all other model results. The multi-model ensemble mean warming rate and amplitude under SRES A2 are 0.45℃ (10 yr)$^{-1}$ and 4.42℃, respectively, largest among the three scenarios. The SRES B1 gives the smallest rate (0.22℃ (10 yr)$^{-1}$) and amplitude (2.60℃), while the rate and amplitude under SRES A1B are 0.39℃ (10 yr)$^{-1}$ and 3.80℃, respectively. The warming over China is consistently greater than the global mean.

The annual mean change in surface air temperature has obvious temporal and geographical variations. As seen in Fig. 2, the multi-model linear tendencies under the three emission scenarios have different features in the early (2011–2030), mid (2046–2065), and late (2080–2099) 21st century. The different scenarios also display common features. The spatial pattern of the change in annual mean surface temperature is

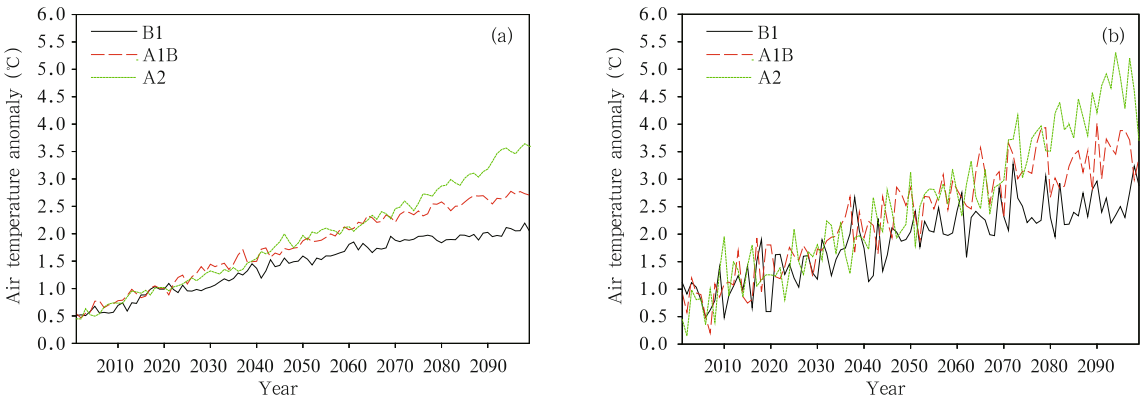

Fig. 1. Surface air temperature (℃) averaged (a) globally and (b) over China, as projected for the 21st century (2001–2099) under the three emission scenarios (SRES B1, A1B, and A2) by BCC_CSM1.0.

Table 3. Linear warming tendency (℃ $(10\ \mathrm{yr})^{-1}$) during the 21st century (2001–2099) and warming amplitude (℃) by the late 21st century (2080–2099) relative to the 1961–1990 mean for surface air temperature averaged globally and over China

Model	SRES B1 (Trend/warming amplitude)		SRES A1B (Trend/warming amplitude)		SRES A2 (Trend/warming amplitude)	
	Globe	China	Globe	China	Globe	China
BCC_CSM1.0	0.17/1.99	0.20/2.52	0.23/2.63	0.30/3.33	0.31/3.24	0.42/4.36
BCCR-BCM2.0	0.16/1.79	0.17/1.90	0.30/2.72	0.32/2.98	0.35/3.17	0.36/3.43
CCSM3	0.11/1.66	0.12/2.14	0.25/2.75	0.33/3.58	0.36/3.70	0.48/4.91
CGCM3.1(T47)	0.15/1.94	0.16/2.30	0.24/2.73	0.28/3.32	0.35/3.51	0.44/4.39
CGCM3.1(T63)	0.19/2.44	0.19/2.60	0.30/3.35	0.34/3.67	–/–	–/–
CNRM-CM3	0.14/1.81	0.17/2.33	0.28/2.81	0.37/3.74	0.38/3.62	0.48/4.66
CSIRO-Mk3.0	0.13/1.27	0.16/1.76	0.21/2.02	0.28/2.75	0.28/2.73	0.35/3.56
ECHAM5/MPI-OM	0.25/2.37	0.37/3.44	0.37/3.38	0.55/4.74	0.40/3.66	0.56/5.06
ECHO-G	0.18/1.92	0.32/3.41	0.31/2.91	0.54/5.05	0.33*/3.22*	0.55*/5.53*
FGOALS-g1.0	0.17/1.83	0.20/1.93	0.27/2.63	0.34/2.96	–/–	–/–
GFDL-CM2.0	0.18/2.11	0.24/2.55	0.30/2.97	0.45/4.05	0.34/3.35	0.51/4.87
GFDL-CM2.1	0.14/1.78	0.21/2.43	0.25/2.65	0.42/4.00	0.31/3.18	0.46/4.43
GISS-AOM	0.13/1.47	0.19/2.33	0.21/2.05	0.31/2.96	–/–	–/–
GISS-EH	–/–	–/–	0.21/2.22	0.30/3.15	–/–	–/–
GISS-ER	0.12/1.52	0.16/2.00	0.21/2.21	0.28/3.03	0.28/2.75	0.38/3.72
INM-CM3.0	0.18/2.13	0.22/3.05	0.24/2.70	0.36/4.07	0.33/3.37	0.48/5.20
IPSL-CM4	0.21/2.37	0.30/3.27	0.32/3.33	0.50/4.79	0.38/3.76	0.55/5.22
MIROC3.2(hires)	0.28/3.28	0.37/4.21	0.43/4.38	0.57/5.57	–/–	–/–
MIROC3.2(medres)	0.22/2.33	0.32/3.40	0.34/3.30	0.48/4.60	0.38/3.68	0.53/5.24
MRI-CGCM2.3.2	0.16/1.70	0.22/2.21	0.25/2.39	0.36/3.17	0.29/2.73	0.38/3.53
PCM	0.10/1.35	0.12/1.62	0.21/2.15	0.28/2.78	0.24/2.43	0.31/3.10
UKMO-HadCM3	0.21/2.15	0.32/3.12	0.31/3.03	0.48/4.44	0.37/3.52	0.55/5.00
UKMO-HadGEM1	–/–	–/–	0.35/3.51	0.47/4.53	–/–	–/–
Multimodel	0.17/1.96	0.22/2.60	0.28/2.82	0.39/3.80	0.33/3.27	0.45/4.42

Notes: Given that the output of ECHO-G under SRES A2 (marked with *) is available only to 2098, the corresponding ensemble mean does not include this model.

generally consistent, with greater warming projected in northern China and less warming in southern China. The two centers of strongest warming are located in northeastern China and over the Qinghai-Tibetan Plateau.

Regardless of the period or phase, the warming tendency is the weakest under SRES B1. Under the other two scenarios, the warming tendency in the earlier period of the 21st century is greater under SRES A1B than under SRES A2, for entire China except for the northeast of China. In the mid and late 21st century, the warming tendency is greater under SRES A2 than under SRES A1B, especially in the late 21st century. Under each scenario, the warming tendencies are different during different stages. Under SRES B1 and A1B, the warming tendencies are greater in the mid 21st century than in the early 21st century, while those in the late 21st century are smaller than either of the earlier two periods. By contrast, under SRES A2, the warming tendency increases with time. These characteristics of air temperature change reflect the atmospheric response to greenhouse gas emissions.

There are substantial uncertainties in the spatial distribution of projected surface air temperature change. Although each model projects a similar increasing trend, the tendencies are geographically different. Zhou and Yu (2006) analyzed the simulation capabilities of 19 CMIP3 models for air temperature over the past 100 years. They found that, given actual external forcing, such as greenhouse gases and aerosols, coupled models are able to reasonably reproduce temperature changes in the 20th century on global, hemispheric, and continental scales. However, there are obvious differences in the spatial distribution

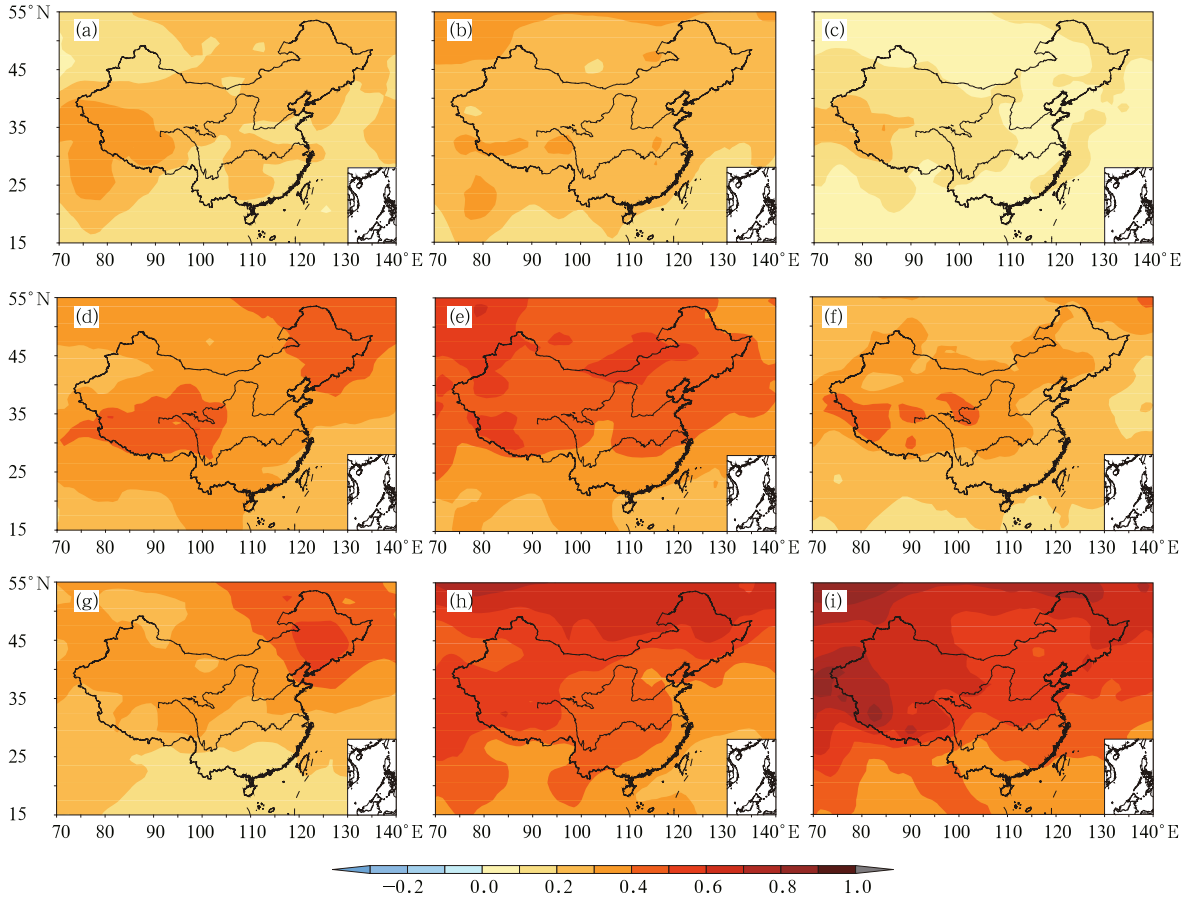

Fig. 2. Linear tendency of surface air temperature (℃ (10 yr)$^{-1}$) during the 21st century according to the multi-model mean under SRES B1 (a–c), A1B (d–f), and A2 (g–i) for the periods 2011–2030 (a, d, g), 2046–2065 (b, e, h), and 2080–2099 (c, f, i).

of warming tendencies between simulations and observations. Although the direct forcing effects of aerosols are considered, almost no model is able to reproduce the cooling trend in summer over eastern China (near 27°–36°N, 100°E) during the recent decades, one of the most significant characteristics in decadal variability over China. The limitation in regional climate simulation suggests that uncertainties exist in the projected distribution of air temperature. Analysis of projections by 23 models under the A1B scenario shows that the projections are credible over most of China, as the signal of the projected change exceeds the deviation among the models (Li and Zhou, 2010). Using the same method, we have analyzed the changes in surface air temperature over the three distinct periods of the 21st century and obtained similar results (figure omitted).

3.2 Annual mean air temperature change in the troposphere and stratosphere

Under global warming during the 20th century, the temperature of the troposphere increased, while the temperature of the stratosphere decreased (IPCC, 2007). Attribution analysis provides some explication (Karl et al., 2006). The increase in greenhouse gas concentrations due to human activities could result in warming of the surface and troposphere and cooling of the stratosphere on the global scale. Decreases in stratospheric ozone lead to a colder lower stratosphere and upper troposphere. Increases in anthropogenic sulfate aerosols may cause regional decreases in surface and tropospheric air temperature. Severe volcanic

eruptions may decrease the surface and tropospheric air temperature for 3–5 yr and increase the stratospheric air temperature for 1–2 yr. Furthermore, increases in solar radiation also contribute to warming throughout the atmosphere. The observed warming of the troposphere and cooling of the stratosphere are comprehensive effects of all the above forcing factors. The analysis of climate change in the 20th century simulated by BCC_CSM1.0 shows that the model is generally able to capture the main characteristics of atmospheric temperature change. This capability indicates that this model may be able to produce the response of the atmosphere to external forcing in the future.

The BCC_CSM1.0 projections indicate that globally-averaged tropospheric air temperatures would increase at different rates under different emission scenarios. The amplitude of warming gradually increases with height from 850 to 300 hPa under each scenario. Similar to surface air temperature, the warming tendency and amplitude are the highest under the A2 scenario, smallest under B1, and moderate under A1B. Above 250 hPa, the warming trend becomes weaker than at lower levels. At 100 hPa, the warming trend becomes very weak. Air temperature decreases from 70 hPa to upper levels, with stronger cooling trends at higher altitudes. Similarly, the stratospheric cooling trend is the largest under A2, intermediate under A1B, and smallest under B1. Comparative analysis shows that the characteristics of tropospheric and stratospheric air temperature change are similar between BCC_CSM1.0 and the CMIP3 models, except for some differences in the trend coefficients.

Here, we analyze possible changes in air temperature over the 21st century averaged globally and over China according to BCC_CSM1.0 and the CMIP3 models at each fixed level.

Figure 3a shows the amplitude of globally-averaged air temperature change at each fixed level for every individual model and the ensemble mean. According to BCC_CSM1.0, the amplitude of the projected warming by the late 21st century increases from 2.57℃ at 850 hPa to 3.37℃ at 300 hPa and then gradually decreases from 250 hPa (3.07℃) to higher levels. The change in air temperature becomes negative at 70 hPa (–0.84 ℃), and the cooling increases with height up to –3.21℃ at 30 hPa. The BCC_CSM1.0 projections are consistent with those from other models.

Figure 3b shows the amplitude of warming averaged over China for each fixed level for each individual model and the ensemble mean. According to BCC_CSM1.0, the amplitude of the projected warming by the late 21st century gradually decreases from 3.38℃ at 850 hPa to 2.89℃ at 600 hPa, and then gradually increases to 3.12℃ at 300 hPa. The air temperature decreases above that level, becoming negative at 70 hPa (–0.23℃), with greater cooling at higher levels. The changes in air temperature over China are smaller than the global average. Comparison among the models shows that the characteristics of air temperature change in the middle and lower troposphere simulated by BCC_CSM1.0 are similar to those simulated by FGOALS-g1.0, INM-CM3.0, MIROC3.2 (medres), and UKMO-HadCM3, but are different from those simulated by most of the other models. The changes are qualitatively similar among all of the models in the upper troposphere and stratosphere, with differences in specific values.

3.3 Annual mean precipitation change

3.3.1 Globally-averaged annual mean precipitation change

Figure 4a shows the time series of globally-averaged annual mean precipitation projected by BCC_CSM1.0 under SRES B1, A1B, and A2. Globally-averaged annual mean precipitation is projected to increase intermittently through the 21st century under all the three emission scenarios, although the trend and amplitude differ under the different scenarios. The increasing trend is larger under SRES A2 (0.63% (10 yr)$^{-1}$) than under A1B (0.46% (10 yr)$^{-1}$) or B1 (0.33% (10 yr)$^{-1}$). The projected changes by the late 21st century are 4.93% under SRES A2, 3.45% under A1B, and 2.53% under B1. Generally, the projected change is the greatest under SRES A2 and smallest under SRES B1.

The change in precipitation projected by BCC_CSM1.0 is within the range of the CMIP3

models' results. The increasing trend and increment of the precipitation over the 21st century are the largest under SRES A2 (0.53% (10 yr)$^{-1}$ and 5.19%, respectively). Under SRES A1B, the trend is 0.45% (10 yr)$^{-1}$ and the increment is 4.40%; under SRES B1, the trend is 0.32% (10 yr)$^{-1}$ and the increment is 3.40%, smallest of the three.

3.3.2 Annual mean precipitation change averaged over China

Figure 4b shows the annual mean relative precipitation anomaly averaged over China, as projected by BCC_CSM1.0 for the 21st century under SRES B1,

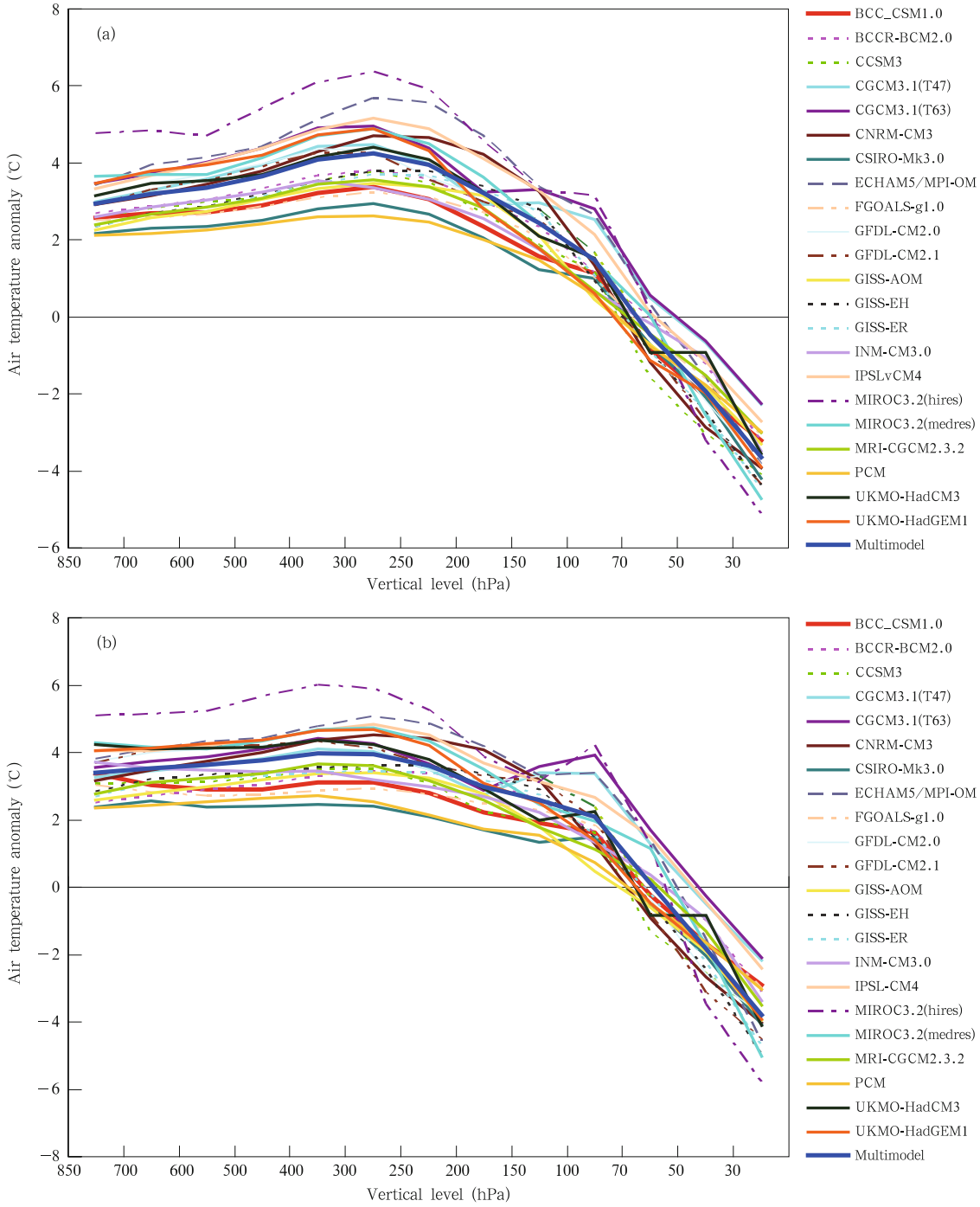

Fig. 3. Annual mean air temperature changes (℃) averaged (a) globally and (b) over China by the late 21st century (2080–2099).

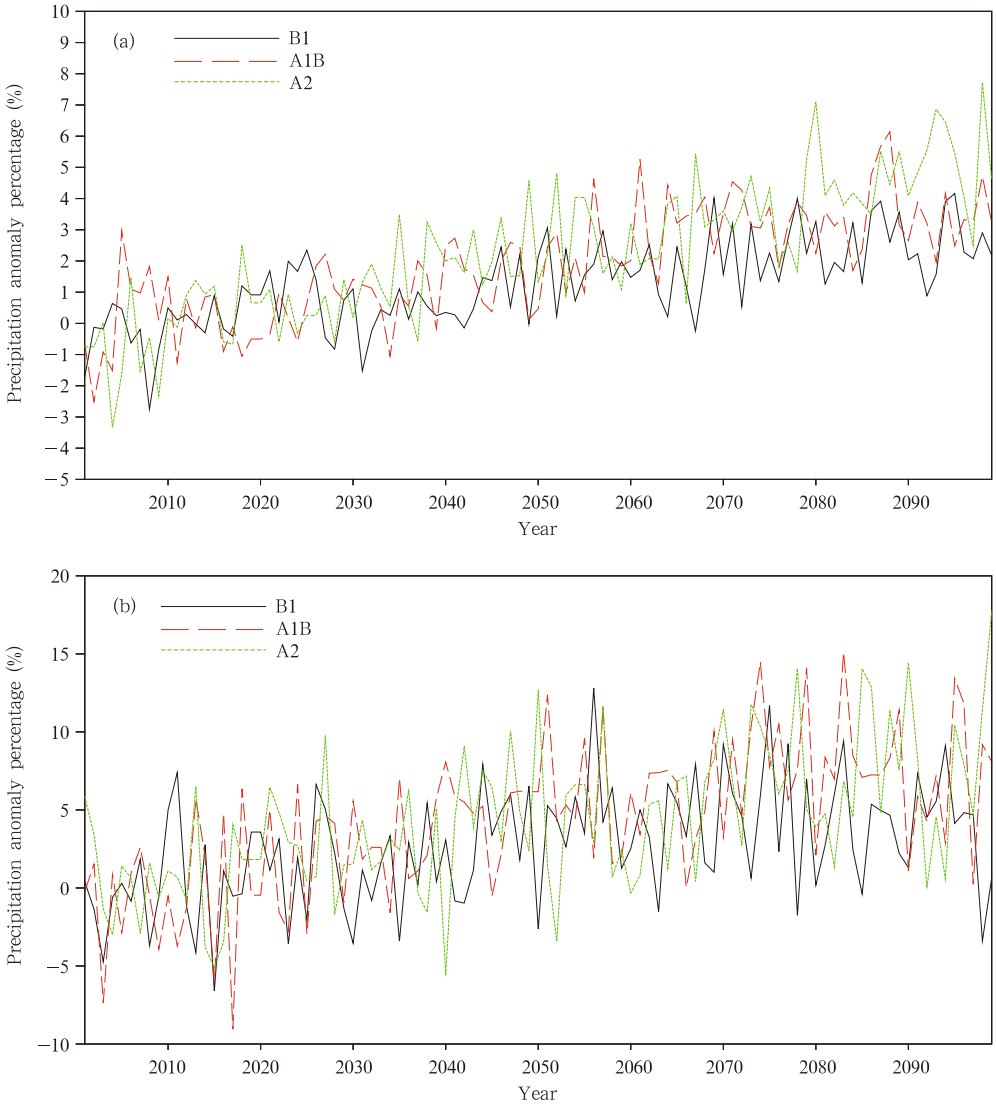

Fig. 4. Annual mean relative precipitation anomaly change averaged (a) globally and (b) over China, as projected by BCC_CSM1.0 for the 21st century under SRES B1, A1B, and A2.

A1B, and A2. Each model projects an intermittent increase in precipitation in the 21st century although the annual variability of China precipitation is larger than the globally-averaged change under all scenarios. The linear tendencies under SRES A2 and A1B are similar, 0.91% (10 yr)$^{-1}$ under SRES A2 and 1.04% (10 yr)$^{-1}$ under SRES A1B. The projected change under SRES B1 is 0.56% (10 yr)$^{-1}$, the smallest of the three. The incremental change over China by the late 21st century is the greatest under A2 (7.60%), intermediate under SRES A1B (7.32%), and smallest under SRES B1 (3.82%). All of these values exceed the global averages.

Comparative analysis reveals that the BCC_CSM1.0 projection is within the range of the CMIP3 model results. According to the ensemble mean, the annual mean relative precipitation anomaly averaged over China increases during the 21st century. The linear tendency is approximately 1.14% (10 yr)$^{-1}$ under SRES A2, larger than those under SRES A1B (1.04% (10 yr)$^{-1}$) or SRES B1 (0.65% (10 yr)$^{-1}$). The increments by the late 21st century are approximately the same under SRES A2 (8.80%) and A1B (8.84%). The increment under SRES B1 is the smallest (6.07%).

Figure 5 shows the annual mean precipitation anomaly change over three distinct periods of the 21st century under the three emission scenarios. The three scenarios have obvious differences in phase and geographical distribution. The ensemble mean indicates a gradual increase in the annual mean precipitation under each of the three emission scenarios, generally with a larger increase in precipitation in northern China and a smaller increase in southern China. There is a large increase in precipitation, extending from northern China to northwestern China through the middle and late periods of the 21st century. In the early 21st century, precipitation is projected to increase over the northern Yellow River basin under all three emission scenarios, with decreases in precipitation over the southern Yellow River basin under SRES A2. In the middle of the 21st century, precipitation is projected to increase over most of the land areas in China under all three scenarios, except the southwestern region under SRES B1 and A2. In the late 21st century, precipitation is projected to increase throughout China under SRES A2, except the southeastern sea.

There are obvious differences in the spatial pattern of precipitation change among the models, indicating substantial uncertainties in the projection of precipitation. The majority of the CMIP3 models cannot reproduce the spatial distribution of heavy precipitation over the last 50 years of the 20th century (Zhang, 2008). Some studies (Feng et al., 2010; Li et al., 2010) show that higher-resolution models provide better simulations of precipitation in eastern China; however, there are still obvious discrepancies in these simulations and projections using a regional climate model for precipitation south of 30°N, where the climate is controlled by monsoon. The consistency among the models regarding the spatial distribution

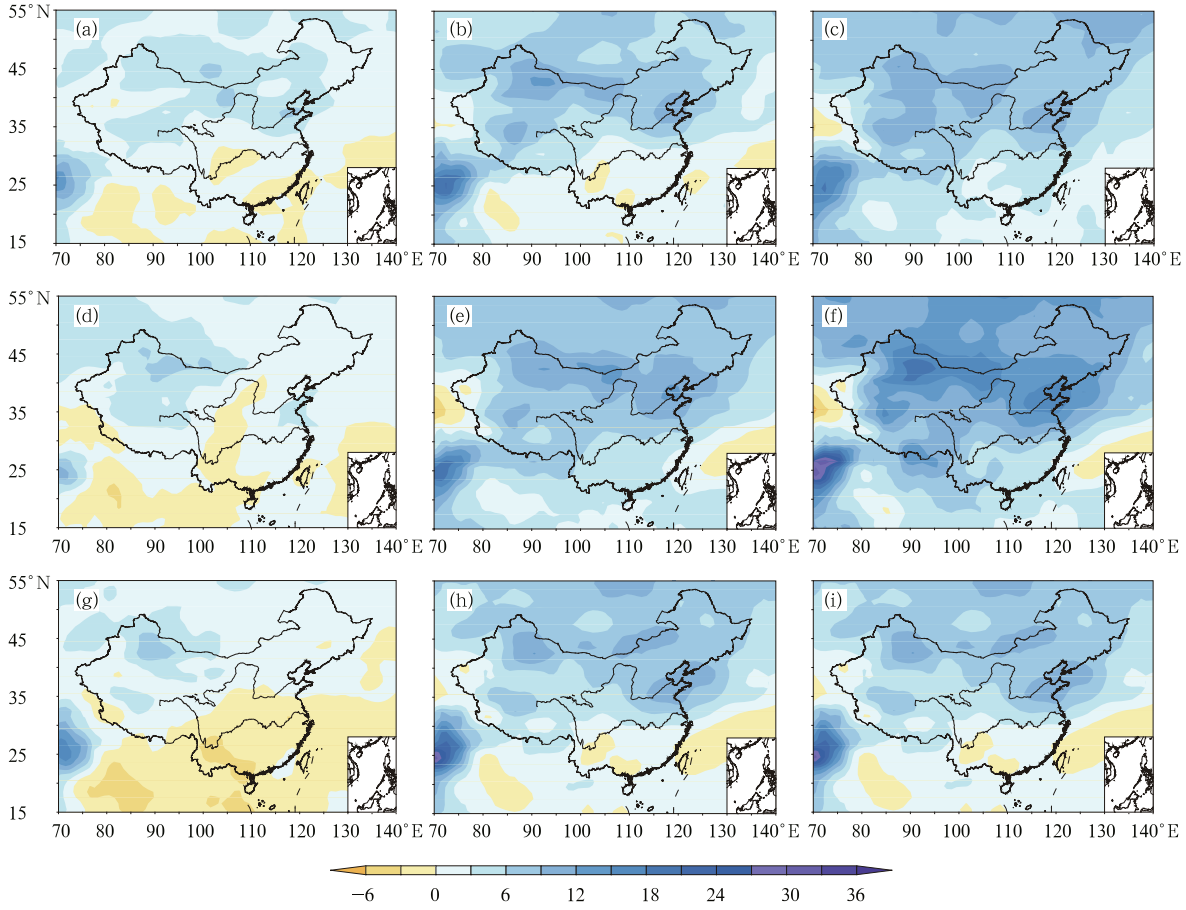

Fig. 5. As in Fig. 2, but for precipitation (% (10 yr)$^{-1}$).

of precipitation changes over the southern Yangtze River basin in the 21st century is very low. All of the models indicate that there are great uncertainties in the projections of future precipitation over the East Asian monsoon region. Using the output from 23 CMIP3 models under SRES A1B, Li and Zhou (2010) found that the uncertainty in projections of precipitation in the middle of the 21st century is larger for the summer mean than for annual or winter means. The ensemble mean signals (annual, summer, and winter) are all smaller than the deviation among the models over China, except for some local regions. We have also calculated the amplitude of the ensemble mean change and standard deviation among models (SDM) for three periods of the 21st century under the three scenarios. The SDM exceeds the change signals over almost all of China in the early 21st century, implying that the changes may not be credible. In the middle and late 21st century, more uncertainties exist southward of 40°N than northward of 40°N (figure omitted).

4. Conclusions and discussion

The above analyses show that the changes in air temperature and precipitation projected for the 21st century by BCC_CSM1.0 are within the range of projections made by other CMIP3 models. The changes in air temperature and precipitation averaged over China are greater than the global means. The results are summarized as follows.

(1) According to the BCC_CSM1.0 projection, annual mean surface temperature averaged globally and over China will increase continuously during the 21st century under SRES A1, A1B, and B1. The warming tendency and amplitude are greater over China than over the globe. The 21st century globally-averaged warming rates are 0.31 ℃ (10 yr)$^{-1}$ for SRES A2, 0.23℃ (10 yr)$^{-1}$ for SRES A1B, and 0.17℃ (10 yr)$^{-1}$ for SRES B1. The warming rates averaged over China are 0.42℃ (10 yr)$^{-1}$ for SRES A2, 0.30℃ (10 yr)$^{-1}$ for SRES A1B, and 0.20℃ (10 yr)$^{-1}$ for SRES B1. By the late 21st century, the amplitude of the globally-averaged warming is 3.24℃ for SRES A2, 2.63℃ for SRES A1B, and 1.99℃ for SRES B1. Averaged over China, the projected warming is 4.36℃ for SRES A2, 3.33℃ for SRES A1B, and 2.52℃ for SRES B1. These results are quite consistent with the ensemble mean values. The enhanced warming over China relative to the global mean is consistent with the output of the CMIP3 models. All of the models consistently project a more pronounced warming trend in western China than in eastern China, and a much more pronounced warming trend in northern China than in southern China.

(2) The annual mean tropospheric air temperature averaged globally and over China is projected by BCC_CSM1.0 to increase in the 21st century under SRES A1B. The air temperature in the stratosphere is projected to decrease at levels above 70 hPa, with greater cooling rates at higher altitudes.

(3) The BCC_CSM1.0 projection indicates that precipitation averaged globally and over China will increase intermittently in the 21st century under all three emission scenarios. As with temperature, the changes in precipitation are more pronounced in China than in the global mean. In the 21st century, the global mean rates of change in annual mean precipitation are 0.63% (10 yr)$^{-1}$ under SRES A2, 0.46% (10 yr)$^{-1}$ under SRES A1B, and 0.33% (10 yr)$^{-1}$ under SRES B1. The rates of change for precipitation averaged over China are 0.91% (10 yr)$^{-1}$ under SRES A2, 1.04% (10 yr)$^{-1}$ under SRES A1B, and 0.56% (10 yr)$^{-1}$ under SRES B1. By the late 21st century, globally-averaged precipitation is projected to increase by 4.93% under SRES A2, 3.45% under SRES A1B, and 3.45% under SRES B1. Average precipitation over China is projected to increase by 7.60% under SRES A2, 7.32% under SRES A1B, and 3.82% under SRES B1. Meanwhile, there are obvious differences in the phase and geographical distribution of precipitation change. The differences in the precipitation change, especially in its spatial distribution, are much larger than the differences in the temperature changes among all of the analyzed models. These differences reflect the greater uncertainties and the lower capability of the models to perform projections of precipitation. Thus, there is still substantial work to be done by the BCC to improve the capability of its climate

system model, especially in the simulation of precipitation.

According to the above analysis, the projection capability of BCC_CSM1.0 is comparable to that of the 22 CMIP3 models. However, we should also consider the defects in BCC_CSM1.0 to better understand its simulation capability. For example, there are no obvious signals of severe volcanic eruptions in the stratosphere in the simulations of historical climate, which may directly affect the credibility of projections of stratospheric air temperature by this model.

The projected changes in annual mean air temperature and precipitation over China are larger than the globally-averaged values according to BCC_CSM1.0, as they are for most of the other CMIP3 models. This pattern of changes indicates that the response of climate over China to an increase in greenhouse gases is much greater than the global mean climate response, and this area may be one of the most susceptible regions. Given this large spatial difference, China should pay additional attention to climate change, and will face greater challenges in dealing with climate change.

Uncertainties in the projections should also be fully considered, especially as regards precipitation. Although consistent conclusions can be drawn from the ensemble mean or even from individual models, the deviation among the models is nonnegligible. In order to make scientific decisions, especially major decisions concerning national development and people's livelihood, the uncertainties in the projections must be reduced. This uncertainty reduction can be accomplished through improvements in the representation of physical processes (e.g., aerosols or cloud physical processes) or improvements in the spatial resolution of the model.

Acknowledgments. We acknowledge the Program for Climate Model Diagnosis and Intercomparison (PCMDI) for collecting and archiving the model data, the Joint Scientific Committee/Climate Variability & Predictability (JSC/CLIVAR) Working Group on Coupled Modeling (WGCM) and their Coupled Model Intercomparison Project (CMIP) and Climate Simulation Panel for organizing the model data analysis activity, and the IPCC Working Group I Technical Support Unit (WGI TSU) for technical support. The IPCC Data Archive at Lawrence Livermore National Laboratory is supported by the Office of Science, U. S. Department of Energy. We thank all scientists working for the development of BCC_CSM1.0. We also thank Dr. Cheng Yanjie for his suggestion.

REFERENCES

Briegleb, B. P., E. C. Hunke, C. M. Bitz, et al., 2004: The sea-ice simulation of the Community Climate System Model Version 2. NCAR Tech. Note NCAR/TN-451STR, 34 pp.

Dickinson, R. E., K. W. Oleson, G. Bonan, et al., 2006: The community land model and its climate statistics as a component of the community climate system model. *J. Climate*, **19**, 2302–2324.

Division of Climate System Modeling (DCSM), 2008: Annual Progress Report for Climate System Model Research and Development (2008). National Climate Center, China Meteorological Administration, 84 pp. (in Chinese)

Dong Min, Wu Tongwen, Wang Zaizhi, et al., 2009: Simulations of the tropical intraseasonal oscillations by the AGCM of the Beijing Climate Center. *Acta Meteor. Sinica*, **67**(6), 912–922. (in Chinese)

Feng Lei, Zhou Tianjun, Wu Bo, et al., 2010: Projection of future precipitation change over China with a high-resolution global atmospheric model. *Adv. Atmos. Sci.*, **28**(2), 464–476.

IPCC, 2001: *Climate Change 2001: The Scientific Basis.* Contribution of Working Group I to the Third Assessment Report of the Intergovernmental Panel on Climate Change. Houghton, J. T., Y. Ding, D. J. Griggs, et al., Eds., Cambridge University Press, Cambridge, United Kingdom and New York, NY, USA, 881 pp.

——, 2007: *Climate Change 2007: The Physical Science Basis.* Contribution of Working Group I to the Fourth Assessment Report of the Intergovernmental Panel on Climate Change. Solomon, S., D. Qin, M. Manning, et al., Eds., Cambridge University Press, Cambridge, United Kingdom and New York, NY, USA, 996 pp.

Jiang Zhihong, Zhang Xia, and Wang Ji, 2008: Projection of climate change in China in the 21st century by IPCC AR4 Models. *Geograph. Res.*, **27**(4), 787–

799. (in Chinese)

Karl, T. R., S. J. Hassol, C. D. Miller, et al., 2006: Temperature Trends in the Lower Atmosphere: Steps for Understanding and Reconciling Differences. A Report by the Climate Change Science Program and Subcommittee on Global Change Research, Washington D. C., 180 pp. http://www.climatescience.gov/Library/sap/ sap1-1/finalreport/default.htm.

Kauffman, B. G., and W. G. Large, 2002: The CCSM Coupler Version Combined User's Guide, Source Code Reference and Scientific Description. National Center for Atmospheric Research, Box 3000, Boulder, CO 80307, USA, 1–46.

Kiehl, J. T., and P. R. Gent, 2004: The Community Climate System Model, version 2. *J. Climate*, **17**, 3666–3682.

Li Bo and Zhou Tianjun, 2010: Projected climate change over China under SRES A1B scenario: Multi-model ensemble and uncertainties. *Adv. Climate Change Res.*, **6**(4), 270–276. (in Chinese)

Li Hongmei, Feng Lei, and Zhou Tianjun, 2011: Multi-model projection of July-August climate extremes changes over China under CO_2 doubling scenario projected by CMIP3 models for IPCC AR4. Part I: Precipitation. *Adv. Atmos. Sci.*, **28**(2), 433–447.

Nakicenovic, N., A. Joseph, D. Gerald, et al., 2000: *Special Report on Emissions Scenarios: A Special Report of Working Group III of the Intergovernmental Panel on Climate Change*. Cambridge University Press, Cambridge, U. K., 599 pp.

Wang Lu, Zhou Tianjun, Wu Tongwen, et al., 2009: Simulation of the leading mode of Asian-Australian monsoon interannual variability with Beijing Climate Center atmospheric general circulation model. *Acta Meteor. Sinica*, **67**(6), 973–982. (in Chinese)

Wu Tongwen, Yu Rucong, Zhang Fang, et al., 2010a: The Beijing Climate Center atmospheric general circulation model: Description and its performance for the present-day climate. *Climate Dyn.*, **34**, 123–147.

——, ——, and ——, 2010b: Modified dynamic framework for the atmospheric spectral model and its application. *J. Atmos. Sci.*, **65**(7), 2235–2253.

Xin Xiaoge, Wu Tongwen, and Wang Zaizhi, 2009: Numerical simulation of climate change in 21 century under two different mitigation scenarios. *Acta Meteor. Sinica*, **67**(6), 935–946. (in Chinese)

Xu Ying, Zhao Zongci, Luo Yong, et al., 2005: Climate change projections for the 21st century by the NCC/IAP T63 with SRES scenarios. *Acta Meteor. Sinica*, **19**, 407–417.

Yu Yongqiang, Zhi Hai, Wang Bin, et al., 2008: Coupled model simulations of climate changes in the 20th century and beyond. *Adv. Atmos. Sci.*, **25**(4), 641–654.

Zhang Li, 2008: Evaluation of AOCGCMs for precipitation simulation in East Asia. Ph. D. Dissertation, Graduate University of the Chinese Academy of Sciences, Beijing, 249 pp. (in Chinese)

——, Dong Min, Wu Tongwen, 2011: Changes in precipitation extremes over eastern China simulated by the Beijing Climate Center Climate System Model (BCC_CSM1.0). *Climate Res.*, **50**, 227–245.

Zhou Tianjun, Yu Yongqiang, Yu Rucong, et al., 2004: Coupled climate system model coupler review. *Chinese J. Atmos. Sci.* **28**(6), 993–1008. (in Chinese)

——, Yu Rucong, Wang Zaizhi, et al., 2005a: *The Atmospheric General Circulation Model SAMIL and the Associated Coupled Model FGOALS_s*. China Meteorological Press, Beijing, 288 pp. (in Chinese)

——, Wang Zaizhi, Yu Rucong, et al., 2005b: The climate system model FGOALS_s using LASG/IAP specral AGCM SAMIL as its atmospheric component. *Acta Meteor. Sinica*, **63**(5), 702–715. (in Chinese)

——, and Yu Rucong, 2006: Twentieth century surface air temperature over China and the globe simulated by coupled climate models. *J. Climate*, **19**, 5843–5858.

——, Yu Yongqiang, Liu Hailong, et al., 2007: Progress in the development and application of climate ocean models and ocean-atmosphere coupled models in China. *Adv. Atmos. Sci.*, **24**(6), 729–738.

——, Wu Bo, Wen Xinyu, et al., 2008: A fast version of LASG/IAP climate system model and its 1000-year control integration. *Adv. Atmos. Sci.*, **25**(4), 655–672.